

This work was written as part of one of the author's official duties as an Employee of the United States Government and is therefore a work of the United States Government. In accordance with 17 U.S.C. 105, no copyright protection is available for such works under U.S. Law.

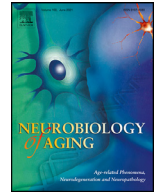
Public Domain Mark 1.0

<https://creativecommons.org/publicdomain/mark/1.0/>

Access to this work was provided by the University of Maryland, Baltimore County (UMBC) ScholarWorks@UMBC digital repository on the Maryland Shared Open Access (MD-SOAR) platform.

**Please provide feedback**

Please support the ScholarWorks@UMBC repository by emailing [scholarworks-group@umbc.edu](mailto:scholarworks-group@umbc.edu) and telling us what having access to this work means to you and why it's important to you. Thank you.



# Plasma neurofilament light as blood marker for poor brain white matter integrity among middle-aged urban adults

May A. Beydoun<sup>a,†,#,\*</sup>, Nicole Noren Hooten<sup>a,#</sup>, Jordan Weiss<sup>b</sup>, Ana I. Maldonado<sup>a,c</sup>, Hind A. Beydoun<sup>d</sup>, Leslie I. Katznel<sup>e,f</sup>, Christos Davatzikos<sup>g</sup>, Rao P. Gullapalli<sup>h</sup>, Stephen L. Seliger<sup>i</sup>, Guray Erus<sup>g</sup>, Michele K. Evans<sup>a</sup>, Alan B. Zonderman<sup>a</sup>, Shari R. Waldstein<sup>c,e,f</sup>

<sup>a</sup> Laboratory of Epidemiology and Population Sciences, Intramural Research Program, National Institute on Aging, National Institutes of Health, Baltimore, MD, USA

<sup>b</sup> Stanford Center on Longevity, Stanford University, Stanford, CA USA

<sup>c</sup> Department of Psychology, University of Maryland, Catonsville, MD, USA

<sup>d</sup> Department of Research Programs, Fort Belvoir Community Hospital, Fort Belvoir, VA, USA

<sup>e</sup> Division of Gerontology, Geriatrics, and Palliative Medicine, Department of Medicine, University of Maryland School of Medicine, Baltimore, MD, USA

<sup>f</sup> Division of Gerontology & Geriatric Medicine, Department of Medicine, University of Maryland School of Medicine, Baltimore, MD, USA

<sup>g</sup> Artificial Intelligence in Biomedical Imaging Laboratory (AIBIL), Perelman School of Medicine, University of Pennsylvania, Philadelphia, PA, USA

<sup>h</sup> Department of Diagnostic Radiology and Nuclear Medicine, University of Maryland School of Medicine, Baltimore, MD, USA

<sup>i</sup> Division of Nephrology, Department of Medicine, University of Maryland School of Medicine, Baltimore, MD, USA

## ARTICLE INFO

### Article history:

Received 10 May 2022

Revised 5 October 2022

Accepted 10 October 2022

Available online 21 October 2022

### Keywords:

Neurofilament Light Chain  
brain magnetic resonance imaging  
white matter integrity  
aging

## ABSTRACT

Plasma neurofilament light chain (NfL)'s link to dementia may be mediated through white matter integrity (WMI). In this study, we examined plasma NfL's relationships with diffusion tensor magnetic resonance imaging markers: global and cortical white matter fractional anisotropy (FA) and trace (TR). Plasma NfL measurements at 2 times ( $v_1$ : 2004–2009 and  $v_2$ : 2009–2013) and ancillary dMRI ( $v_{scan}$ : 2011–2015) were considered ( $n=163$ , mean time  $v_1$  to  $v_{scan}=5.4$  years and  $v_2$  to  $v_{scan}$ : 1.1 years). Multivariable-adjusted regression models, correcting for multiple-testing revealed that, overall, higher NfL $_{v_1}$  was associated with greater global TR ( $\beta \pm SE$ :  $+0.0000560 \pm 0.0000186$ ,  $b=0.27$ ,  $p=0.003$ ,  $q=0.012$ ), left frontal WM TR ( $\beta \pm SE$ :  $+0.0000706 \pm 0.0000201$ ,  $b \pm 0.30$ ,  $p=0.001$ ,  $q=0.0093$ ) and right frontal WM TR ( $\beta \pm SE$ :  $+0.0000767 \pm 0.000021$ ,  $b \pm 0.31$ ,  $p < 0.001$ ,  $q=0.0093$ ). These associations were mainly among males and White adults. Among African American adults only, NfL $_{v_2}$  was associated with greater left temporal lobe TR. “Tracking high” in NfL was associated with reduced left frontal FA (Model 2, body mass index-adjusted:  $\beta \pm SE$ :  $-0.01084 \pm 0.00408$ ,  $p=0.009$ ). Plasma NfL is a promising biomarker predicting future brain white matter integrity (WMI) in middle-aged adults.

Published by Elsevier Inc.

## 1. Introduction

Recent technological advances have led to substantial interest in utilizing blood-based markers of neuroaxonal damage to

ported by the [National Institutes of Health, R01-AG034161](#) and [P30 AG028747-14S1](#) to S.R.W. ZIA-AG000513 to M.K.E. and A.B.Z., and The University of Maryland Claude D. Pepper Older Americans Independence Center (NIH grant P30 AG028747).

**Financial disclosure statement:** The authors declare no conflict of interest.

\* Corresponding author at: NIH Biomedical Research Center, National Institute on Aging, IRP, 251 Bayview Blvd., Suite 100, Room #: 04B118, Baltimore, MD 21224. Tel.: 919-423-1087. Fax: 410-558-8236.

E-mail address: [baydounm@mail.nih.gov](mailto:baydounm@mail.nih.gov) (M.A. Beydoun).

† MAB had full access to the data used in this manuscript and completed all the statistical analyses.

# Co-first authors

**Abbreviations:** ADC, Apparent Diffusion Coefficient; CSF, Cerebrospinal Fluid; CV, Coefficient of Variation; C-TRIM, Core for Translational Research in Imaging @ Maryland;  $\delta$ , annualized change; DTI, Diffusion Tensor Imaging; DWI, Diffusion-weighted imaging; FDR, False Discovery Rate; FLAIR, Fluid-Attenuated Inversion Recovery; FA, Fractional Anisotropy; FOV, Field of View; GM, Gray Matter; HANDLS study, Healthy Aging in Neighborhoods of Diversity across the Life Span;  $v_{scan}$ , HANDLS SCAN visit; HS, High School; IRB, Institutional Review Board; ICV, Intracranial Volume; jLMMSE, Joint Linear Minimum Mean Squared Error; MD, Mean diffusivity; MP-RAGE, Magnetization prepared rapid gradient echo; MRI, Magnetic Resonance Imaging; MRV, Medical Research Vehicle; MMSE, Mini-Mental State Examination; MICO, Multiplicative intrinsic component optimization; MUSE, Multi-atlas region Segmentation utilizing Ensembles; NfL, Neurofilament Light; ROI, Regions of Interest; sMRI, Structural MRI; TBV, Total Brain Volume; TR, Trace; US, United States;  $v_1$ , Visit 1;  $v_2$ , Visit 2; WM, White Matter; WMI, White Matter Integrity.

**Sources of funding:** This work was supported in part by the Intramural Research Program of the NIH, National Institute on Aging. This work was also sup-

monitor brain health and health outcomes (Hansson et al., 2017; Khalil et al., 2018; Raket et al., 2020). One of these markers, neurofilament light (NfL), is released into the extracellular space upon axonal damage (Hansson et al., 2017; Khalil et al., 2018; Raket et al., 2020). From this space it migrates to the cerebrospinal fluid (CSF), and subsequently into the blood (Hansson et al., 2017; Khalil et al., 2018; Raket et al., 2020). The ability to reliably detect and monitor blood levels of NfL is advantageous over its CSF counterpart, given that collection of CSF requires invasive procedures, and produces limited sample quantities, resulting in a reluctance to perform multiple lumbar punctures for the acquisition of longitudinal samples (Hansson et al., 2017; Khalil et al., 2018; Raket et al., 2020). It is important to note that several studies have reported a strong correlation between CSF and blood based (serum or plasma) NfL levels, which indicates that blood NfL may have clinical utility as an indicator of neuroaxonal damage (Hansson et al., 2017; Khalil et al., 2018; Raket et al., 2020).

Accumulating data indicates that elevated blood NfL levels are associated with various neurodegenerative diseases (Khalil et al., 2018) including both late and early stages of Alzheimer's dementia (AD) (de Wolf et al., 2020; Mattsson et al., 2019; Preische et al., 2019; Weston et al., 2019), frontotemporal degeneration (Scherling et al., 2014), multiple sclerosis (Teunissen et al., 2005), and traumatic brain injury (Shahim et al., 2016). Most recently, plasma NfL levels have been assessed in community-dwelling cohorts to determine whether this marker can be detected prior to the onset of dementia and in the absence of neurological disease. Blood NfL levels were associated with cognitive performance tests in a middle-aged racially diverse cohort (Beydoun et al., 2021) and with cognitive performance in non-demented older adults (He et al., 2020; Khalil et al., 2020; Mielke et al., 2019; Rajan et al., 2020; Rubsamen et al., 2021). Thus far, there are limited studies examining plasma NfL and subclinical brain structural changes in non-diseased cohorts. However, existing data indicates that higher NfL levels during normal aging are associated with brain atrophy (Khalil et al., 2020; Mielke et al., 2019; Rajan et al., 2020; Rubsamen et al., 2021). Therefore, there is a need to identify in middle-aged adults, predictors of brain health for later in life, especially in diverse cohorts.

In order to establish blood NfL as an indicator of brain health, it is important to characterize the relationship of NfL levels with brain microstructural abnormalities detected using various imaging modalities. One of these methods, Diffusion-Weighted Imaging (DWI), is a variant of conventional MRI that targets the diffusion rate of tissue water (Soares et al., 2013). As a non-invasive method, it is highly sensitive to water movements within tissue architecture, and makes use of existing technologies, with no additional requirement, such as new equipment, contrast agents or chemical tracers. The diffusion tensor model was later introduced to obtain an indirect measurement of the degree of anisotropy and structural orientation specific to diffusion tensor imaging (DTI) (Soares et al., 2013). DTI posits that water molecules diffuse in different ways along tissues, a pattern that depends in part on tissue type, integrity, architecture and barriers, which yields data about the tissue's orientation and its quantitative anisotropy (Soares et al., 2013). In fact, water diffusion along the axon tends to be directionally-dependent and thus anisotropic, whereas it is less so in gray matter and completely unrestricted in the CSF and in all directions (Soares et al., 2013). DTI is a powerful tool to analyze brain microstructural details including white matter tracts and white matter integrity. With DTI analysis it is now possible to determine at the voxel level, several properties including the directional preference of diffusion [Fractional Anisotropy (FA)], molecular diffusion rate [Trace, TR], and Mean diffusivity (MD) also known as Apparent Diffusion Coefficient (ADC)] (Soares et al.,

2013). Fractional Anisotropy (FA) is a widely established method for quantifying white matter integrity (WMI) that is sensitive to the degree of myelination, density, and organization of WM (Jones, 2008). Specifically, FA determines directionality of water diffusion in the brain, measuring the degree of anisotropy of the diffusion at the voxel level (Jones, 2008). Therefore, FA and TR are both sensitive methods to detect even subtle abnormalities in WM that may not be detected at the anatomical level.

There are a few recent studies that have examined the potential relationship between plasma NfL and brain diffusion white matter integrity (WMI) markers in older White cohorts (Mielke et al., 2019; Nyberg et al., 2020), but in these studies differences were not examined by sex or race. Furthermore, little is known about the association of time-dependent measures of NfL and their relation to brain diffusion WMI markers, especially in non-demented adults. Thus, our present retrospective study (i) Examined time-dependent plasma NfL in relation to follow-up brain WMI outcomes, including global and cortical regional FA and TR (ii) Examined tracking in NfL in relation to these brain WMI outcomes at follow-up; (iii) Tested sex and race as potential effect modifiers of these associations.

## 2. Methods and materials

### 2.1. Study sample

We used data from the Healthy Aging in Neighborhoods of Diversity across the Life Span (HANDLS) study, an ongoing and prospective, community-based bi-racial cohort study designed to examine age-related health changes among a sample of socioeconomically diverse African American and White adults in Baltimore, MD (Evans et al., 2010). The initial recruitment and examination were composed of 2 phases. In Phase 1, study investigators conducted in-home surveys with participants to collect demographic, psychosocial, and dietary information. During Phase 2, participants were examined in Medical Research Vehicles (MRVs) parked in close proximity to their neighborhoods (Evans et al., 2010). Through the MRV exams, study investigators assessed physical, psychosocial, and medical characteristics. This included, for example, Dual X-ray absorptiometry to measure body composition and bone mineral density, an electrocardiogram, personal and family health history, and physical and neuropsychological tests, (Evans et al., 2010). Serum and plasma specimens were also collected. Phases 1 and 2 data are labelled as visit 1 ( $v_1$ , 2004–2009). Comparable follow-up MRV visits were conducted, including at visit 2 ( $v_2$ , 2009–2013).

In this retrospective analysis of the HANDLS study, participants with complete and valid dMRI data at the HANDLS SCAN visit and complete data at  $v_1$  and  $v_2$  were included (Figure 1). HANDLS SCAN ( $v_{scan}$ , 2011–2015) recruited participants from consecutive waves of first and second follow-up examinations of whom 238 had usable MRI data (e.g., no clinical incidental findings). Of those,  $n=212$  had complete dMRI measures and a measure of intracranial volume (ICV). HANDLS SCAN exclusions were the following: (i) self-reported histories of HIV, neurological, and/or terminal diseases, stroke, transient ischemic attack or carotid endarterectomy or (ii) specific MRI contraindications (e.g., indwelling ferromagnetics). The final sample recruited into HANDLS SCAN was representative of the overall HANDLS study sample in educational attainment, poverty status, and sex ( $p > 0.05$ ); however, HANDLS SCAN participants were more likely to be white and younger ( $p < 0.05$ ).

Plasma NfL data from 2 visits ( $v_1$ : 2004–2009;  $v_2$ : 2009–2013) were thereby analyzed in relation to follow-up data measured among a sub-sample of participants within the HANDLS SCAN sub-study ( $v_{scan}$ : 2011–2015) (Waldstein et al., 2017). This is therefore

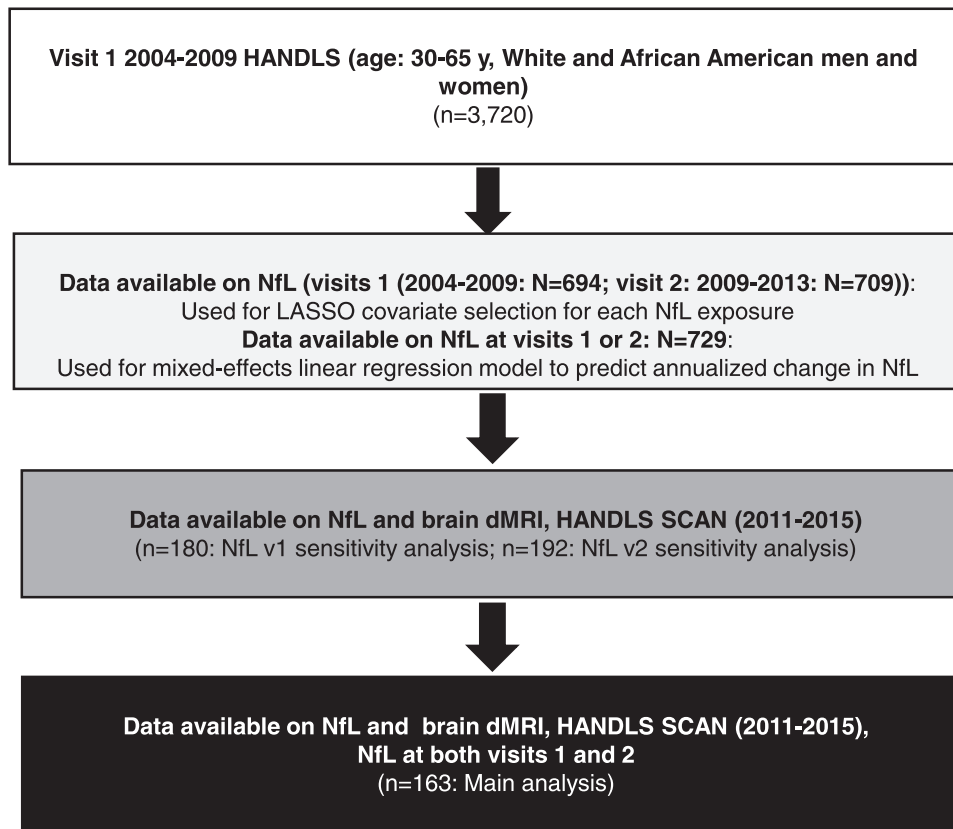


**Fig. 1.** Study participant schematic: HANDLS 2004–2013 and HANDLS-SCAN 2011–2015<sup>a</sup>. Abbreviations: dMRI, Diffusion weighted Magnetic Resonance Imaging; HANDLS, Healthy Aging in Neighborhoods of Diversity Across the Life Span. <sup>a</sup>Visit 1 refers to HANDLS 2004–2009; Visit 2 refers to HANDLS 2009–2013; and HANDLS-SCAN visit ( $v_{scan}$ ) was carried out between 2011 and 2015.

a cross-sectional analysis of a retrospective cohort study, with outcomes measured at 1 time point, that is MRI assessments obtained from  $v_{scan}$  reflecting WMI, and exposures measured as part of the MRV visits at 2 time points ( $v_1$ : 2004–2009 or  $v_2$ : 2009–2013). Mean $\pm$ SD follow-up time between  $v_1$  and  $v_{scan}$  was  $5.61y \pm 1.90$ .

Sample selection is shown in Fig. 1. Data was available for 694 HANDLS participants for NfL $v_1$  and 709 at NfL $v_2$ . These subsamples were used for the least absolute shrinkage and selection operator (LASSO) covariate selection (See *Supplemental Method 4*) and were subsequently restricted to participants having complete data on NfL at both  $v_1$  and  $v_2$ , as well as HANDLS SCAN dMRI and ICV data ( $n=212$ ), yielding a final sample of 163 participants. This final sample ( $N=163$ ), when compared with the remaining excluded participants from the initial sample ( $n=3720$ ), had higher proportions of White adults (59% vs. 40% in excluded sample,  $p < 0.05$ ) and individuals living above poverty (68% vs. 58% in excluded sample,  $p < 0.05$ ).

Written informed consent was provided by all participants. HANDLS and HANDLS SCAN study protocols received approval from the National Institute on Environmental Health Sciences Institutional Review Board (IRB) of the National Institutes of Health. Moreover, HANDLS SCAN protocol was approved by the IRBs of the University of Maryland School of Medicine and the University of Maryland, Baltimore County.

## 2.2. Brain dMRI: WMI measures

dMRI was assessed using multi-band spin echo EPI sequence with a multi-band acceleration factor of 3. FA and TR images were evaluated from tensor images, with higher FA values in-

dicating healthier WMI, and were calculated in the original image space. Summation of eigenvalues for diffusion tensor yields TR, with higher values suggesting poorer WMI, while MD is TR/3 (Jones, 2008). Computed FA and TR images were aligned to a common template space using deformable registration with a standard dMRI template (i.e., MUSE (Doshi et al., 2016)), for the purpose of visualization. More specifically, isotropic resolution images were obtained with an in-plane resolution of  $2 \times 2$  mm and 2 mm slice thickness over a 22.4 cm FOV. A total of 66 slices at a TE = 122ms, TR = 3300ms, and flip angle =  $90^\circ$  were used. Eddy current effects were reduced by using bipolar diffusion. Diffusion-weighting scheme was a 2-shell ( $b=1000, 2500$ ), optimized for uniform sampling of each shell and non-overlapping diffusion directions of 60 and 120, respectively, and 6 b0 volumes. Image acquisition time was ten minutes. Joint Linear Minimum Mean Squared Error software, (jLMMSE; Tristan-Vega and Aja-Fernandez, 2010) was used to de-noise the raw DWI data. The DT images were reconstructed by fitting the de-noised DWI data using multivariate linear fitting. Motion correction was conducted with FSL's "eddycorrect" tool (Andersson and Sotiropoulos, 2016), (*Supplemental Method 1*). *Supplemental Table 1* for lists of ROIs included in our secondary analyses of ROI-specific FA and TR. Global FA and TR were computed as the average across all WM ROIs. Selection of cortical WM subregions that comprised the bilateral (left/right) larger brain regions (Frontal, Temporal, Parietal, Occipital) was similar to previous studies (see Roalf et al., 2015; Shaked et al., 2019). While FA is unitless, TR is measured in  $mm^2/sec$ . *Supplemental Method 1* also details sMRI imaging techniques from which the intracranial volume was estimated.

### 2.3. NfL at $v_1$ and $v_2$

We provide details on the assay procedures for NfL <sub>$v_1$</sub>  (baseline NfL measured at  $v_1$  [2004–2009]) and NfL <sub>$v_2$</sub>  (first follow-up NfL measured at visit  $v_2$  [2009–2013]) in *supplemental Method 2*. We consider both Log<sub>e</sub> transformed NfL <sub>$v_1$</sub>  and NfL <sub>$v_2$</sub>  as primary exposures of interest. As a secondary exposure, we consider a binary marker indicating changes in NfL between  $v_1$  and  $v_2$  as defined by a common median level of untransformed plasma NfL (i.e., >median at both visits for “tracking high” (=1) versus all others (=0); and ≤median value at both visits (=1), for “tracking low” versus all others (=0)). We present results for analyses using this secondary exposure for selected outcomes for which at least 1 of 2 previous exposure-outcome relationships was found to be statistically significant. In addition, for descriptive purposes, we report the  $\delta$ NfL as the annualized rate of change between NfL <sub>$v_1$</sub>  and NfL <sub>$v_2$</sub>  measurements after Log<sub>e</sub> transformation (Beydoun et al., 2021) (see *supplemental method 3*).

### 2.4. Covariates

All covariates used in our analyses were measured during visit 1. We included age (y), sex (male, female), self-identified race (African American, White), self-reported household income (<125% or ≥125% of the 2004 Health and Human Services poverty guidelines HHH 2019 [termed poverty status] ), and time (days) between  $v_1$  MRV visit and  $v_{scan}$ . For our primary analysis, we also included a measure of ICV among potential confounders. We sequentially adjusted for additional covariates which were selected for their potential association with NfL exposures. Details on our modeling procedures are provided in the following section and the *online supplemental method 4*.

### 2.5. Statistical analysis

Using Stata version 16.0 (STATA, 2019) for all analyses, we computed means and proportions of sample characteristics, and tested for sex and race differences using Student's *t* and chi-square tests, as appropriate. We further described the sample characteristics by tertiles of Log<sub>e</sub> transformed NfL <sub>$v_1$</sub>  and NfL <sub>$v_2$</sub>  (*Supplemental Table 2*). Multivariable regression models were subsequently estimated with sequential covariate adjustment, for the complete sample and sex-stratified, including each of 2 exposures predicting dMRI outcome measured at  $v_{scan}$ . We also obtained estimates of standardized *b* which we interpreted as the fraction of a 1 SD change in dMRI outcome per 1 SD change in the specified continuous exposure (i.e., NfL at  $v_1$  and  $v_2$ ). A priori, we classified standardized *b* estimates >0.20 as moderate-to-strong, and estimates between 0.10 and 0.20 as weak to moderate.

We conducted our analysis in 3 stages. Our first analysis (*Analysis A*) included measures of global mean FA (FA<sub>global</sub>) and global mean TR (TR<sub>global</sub>). *Analysis A'*, was a post-hoc regional analysis for *Analysis A* that detailed cortical FA and TR (i.e., as left/right; FA/TR; frontal, temporal, parietal and occipital), thereby yielding 16 post-hoc outcomes. Results from *Analysis A'* were only presented if, for a given model, at least 1 *Analysis A* exposure-outcome association was statistically significant ( $p_{uncorr} < 0.05$ ) in a given sample. Subsequent to *A'*, another secondary analysis was presented for smaller regions of interest (i.e., 19 small and large ROIs) (*Analysis A''*), considers bilateral ROI-specific FA and TR as alternative outcomes of interest (Table S1).

A series of scatter plots were used to visualize findings from ROI-specific models, mainly using 95% CI of effect sizes *b* of exposures from *Model 1*. Visualization of ROI-specific *b* with

standard brain images was accomplished using FSLeys software (Jenkinson et al., 2002; Jenkinson and Smith, 2001) applied to these same dMRI ROI-specific FA/TR results from *Model 1* (URL: <https://fsl.fmrib.ox.ac.uk/fsl/fslwiki/FSLeys>). Although main models adjusted for ICV, a sensitivity analysis was conducted whereby analyses were re-run excluding ICV among potential confounders. We further replicated all our analyses by stratifying the sample by sex and race. Effect modification by sex and/or race was tested using 2-way interactions in the unstratified model at a type I error rate of 0.10.

Type I error was set at 0.05 for uncorrected *p*-values. We corrected for multiple testing using the false discovery rate (FDR, *q*-value). Each stage of analysis conducted for the overall and stratified samples were treated as separate hypotheses (i.e., *Analyses A* and *A'*: overall vs. stratified by sex). In doing so, we adjusted for multiplicity within analysis and across strata. We used this correction specifically for the model with minimal covariate adjustment (i.e., *Model 1*) for each of *Analyses A* and *A'*. We reported FDR *q*-values when  $p_{uncorr} < 0.05$  for exposure-outcome associations. Statistical significance in *Model 1* was determined when FDR *q*-value < 0.05, while a *q*-value < 0.10 but ≥ 0.05 suggested a trend. Our models with sequential covariate adjustment (*Models 2–6*) were presented as secondary analyses designed to test mediating pathways between exposures and outcomes of interest (*online supplemental method 4*). Those covariates were imputed (5 imputations, 10 iterations) using chained equations. Another sensitivity analysis was conducted in the sub-sample that was free from self-reported head injuries at first-visit and was considered as being free from suspected dementia at  $v_1$  based on the Mini-Mental State Examination (MMSE) total score being ≥ 23, ( $n = 147$ ). It is worth noting that no comprehensive dementia screening was available in the HANDLS parent study.

## 3. Results

Study sample characteristics are described in *Table 1*, overall, by sex and by race. The selected analytic sample consisted of 74 males and 89 females, 97 White and 66 African American adults, with mean ± SD age of 47.9 ± 9.1 years, of whom 68.1% were living above poverty (vs. below poverty). Lengths of follow-up ( $v_1$  to  $v_{scan}$  and  $v_2$  to  $v_{scan}$ ), age, race, poverty status as well as key NfL exposures did not differ between males and females. In contrast, males were at higher risk for pre-diabetes compared with females, while also having significantly higher levels of urinary specific gravity, serum uric acid and serum creatinine, and higher serum albumin compared with females. While ICV was larger in men, as expected, there were no sex differences in any of the main WMI measures. African American adults who were selected were significantly younger than their White counterparts (46.1 vs. 49.1 y). However, the difference was no longer significant upon adjustment for sex and poverty status. There were some differences in biochemical and hematologic markers that were selected as potential confounders, most notably reduced blood urea nitrogen and 25-hydroxyvitamin D levels among African American compared with White adults.

We also tested racial differences in NfL and neuroimaging measurements. Importantly, African American adults had lower NfL at  $v_1$  and  $v_2$  compared to White adults, though annualized change in NfL did not differ between the 2 racial groups. “NfL tracking high” (i.e., remaining above median over time), percentage was also higher among White adults. In contrast, global FA was lower among African American adults, indicating lower WMI, in the left parietal and occipital lobes, the right frontal lobe ( $p < 0.010$ ) and the right parietal lobe ( $p = 0.011$ ). Following a similar analytic ap-

**Table 1**  
Study sample characteristics of eligible study sample by sex and by race; HANDLS (v<sub>1</sub>: 2004–2009; v<sub>2</sub>: 2009–2013) and HANDLS-SCAN 2011–2015<sup>a</sup>

	Total (N = 163)	Females (N = 89)	Males (N = 74)	<i>p</i> <sub>sex</sub>	White adults (N = 97)	African American adults (N = 66)	<i>P</i> <sub>race</sub>
Socio-demographic, lifestyle and health-related factors at v <sub>1</sub>							
Sex, % males	45.4	—	—	—	44.3	46.9	0.74
Age <sub>v1</sub>	47.9 ± 9.1	47.4 ± 1.01	48.4 ± 1.01	0.49	49.1 ± 0.87	46.1 ± 1.19	0.042 <sup>b</sup>
Race, % African American	40.5	39.3	41.9	0.74	—	—	—
% above poverty	68.1	62.8	75.7	0.058	71.1	63.6	0.31
Time between v <sub>1</sub> and v <sub>scan</sub> (years)	5.35 ± 1.68	5.38 ± 0.18	5.31 ± 0.19	0.80	5.17 ± 0.19	5.62 ± 0.17	0.11
Time between v <sub>2</sub> and v <sub>scan</sub> (years)	1.07 ± 1.17	1.13 ± 0.13	1.01 ± 0.14	0.54	1.13 ± 0.12	0.99 ± 0.14	0.45
<i>Imputed covariates, % or Mean±SE</i>							
Body mass index, kg.m <sup>-2</sup>	29.3 ± 0.5	30.1 ± 0.8	28.3 ± 0.6	0.087	29.1 ± 0.7	29.5 ± 0.8	0.74
Diabetes							
No	72.5	79.8	63.8	—	71.1	75.0	—
Pre-diabetes	16.9	11.2	23.8	0.029	19.6	31.0	0.33
Diabetes	10.6	9.0	12.4	0.29	9.3	12.0	0.64
Plasma glucose, mg/dL	100.0 ± 2.3	96.1 ± 2.4	104.7 ± 4.1	0.059	102.6 ± 3.3	96.2 ± 2.9	0.17
Creatinine, mg/dL	0.89 ± 0.02	0.80 ± 0.03	1.01 ± 0.03	<0.001	0.88 ± 0.02	0.92 ± 0.04	0.29
Urine Specific Gravity	1.0192 ± 0.0005	1.0180 ± 0.0006	1.0206 ± 0.0007	0.009	1.02 ± 0.00	1.0192 ± 0.0008	0.92
Blood urea nitrogen, mg/dL	13.78 ± 0.33	13.31 ± 0.42	14.33 ± 0.53	0.13	14.84 ± 0.45	12.23 ± 0.43	<0.001
Alkaline Phosphatase, U/L	74.4 ± 1.6	76.2 ± 2.2	72.2 ± 2.3	0.21	75.0 ± 2.0	73.6 ± 2.6	0.65
Uric acid, mg/dL	5.50 ± 0.12	4.97 ± 0.15	6.14 ± 0.16	<0.001	5.46 ± 0.15	5.57 ± 0.19	0.65
Albumin, g/dL	4.34 ± 0.02	4.28 ± 0.03	4.41 ± 0.03	0.001	4.35 ± 0.03	4.32 ± 0.03	0.43
Eosinophils, %	2.75 ± 0.16	2.54 ± 0.23	3.01 ± 0.22	0.14	3.01 ± 0.22	2.38 ± 0.23	0.05
25-hydroxyvitamin D, ng/mL	22.3 ± 0.8	21.7 ± 1.26	23.0 ± 1.3	0.54	26.5 ± 1.0	16.1 ± 1.1	<0.001
Current drug use, % yes	19.6	23.1	15.4	0.25	15.0	27.0	0.06
Self-rated health, %							
Poor/fair	22.1	25.8	17.6	—	20.6	24.0	—
Good	38.7	39.3	37.8	0.42	39.2	38.0	0.64
Very good/Excellent	39.3	34.8	44.6	0.14	40.2	38.0	0.60
%, Mean ± SD							
NfL, Log <sub>e</sub> transformed (v <sub>1</sub> )							
Mean±SD	+2.03 ± 0.53	2.00 ± 0.05	2.07 ± 0.07	0.39	2.14 ± 0.05	1.87 ± 0.07	0.001
Median	1.97	1.97	1.98	—	2.05	1.89	—
IQR	1.70;2.27	1.65;2.27	1.76;2.26	—	1.81; 2.45	1.56;2.19	—
NfL, Log <sub>e</sub> transformed (v <sub>2</sub> )							
Mean±SD	2.23 ± 0.58	2.18 ± 0.06	2.28 ± 0.07	0.30	2.33 ± 0.05	2.08 ± 0.08	0.006
Median	2.18	2.18	2.17	—	2.27	2.05	—
IQR	1.87;2.56	1.82;2.56	1.94; 2.52	—	1.99;2.64	1.66;2.35	—
δNfL, Log <sub>e</sub> transformed, annualized (v <sub>2</sub> -v <sub>1</sub> )							
Mean±SD	+0.044 ± 0.113	+0.044 ± 0.009	0.040 ± 0.015	0.80	0.045 ± 0.011	0.038± 0.014	0.72
Median	+0.043	+0.043	+0.041	—	0.043	0.043	—
IQR	-0.010;+ 0.091	-0.012;0.092	+0.002;0.090	—	-0.004;0.094	-0.017;0.086	—
“Tracking high” v <sub>1</sub> through v <sub>2</sub> : NfL>8 pg/mL	35.6	34.8	36.5	0.82	43.3	24.2	0.013
“Tracking low”, v <sub>1</sub> through v <sub>2</sub> : NfL≤8 pg/mL	36.2	36.0	36.5	0.94	29.9	45.5	0.042
dMRI measures, mm <sup>3</sup>	(N = 163)	(N = 89)	(N = 74)	—	(N = 97)	(N = 66)	—
<i>Global white matter integrity measures</i>							
Mean fractional anisotropy (FA <sub>global</sub> )	0.4276 ± 0.0203	0.428 ± 0.002	0.427 ± 0.002	0.58	0.431 ± 0.002	0.423 ± 0.002	0.015
Mean of trace (TR <sub>global</sub> ), mm <sup>2</sup> /sec	0.00231 ± 0.00011	0.00232 ± 0.00001	0.00231 ± 0.00001	0.71	0.00230 ± 0.00001	0.00230 ± 0.00001	0.74
<i>Regional cortical white matter integrity measures</i>							
<i>Cortical Fractional anisotropy</i>							
<i>Left Brain</i>							
Frontal	0.4123 ± 0.0238	0.4136 ± 0.0026	0.4109 ± 0.0026	0.48	0.4149 ± 0.0024	0.4085 ± 0.0030	0.09
Temporal	0.4171 ± 0.0207	0.4183 ± 0.0023	0.4156 ± 0.0023	0.40	0.4185 ± 0.0021	0.4151 ± 0.0026	0.31
Parietal	0.4222 ± 0.0227	0.4250 ± 0.0026	0.4188 ± 0.0023	0.082	0.4265 ± 0.0024	0.4159 ± 0.0025	0.003
Occipital	0.3974 ± 0.0255	0.3987 ± 0.0027	0.3958 ± 0.0030	0.47	0.4029 ± 0.0027	0.3894 ± 0.0026	<0.001
<i>Right Brain</i>							
Frontal	0.4215 ± 0.0249	0.4214 ± 0.0027	0.4216 ± 0.0027	0.96	0.4261 ± 0.0025	0.4147 ± 0.0030	0.004
Temporal	0.4207 ± 0.0220	0.4220 ± 0.0025	0.4191 ± 0.0024	0.41	0.4218 ± 0.0023	0.419 ± 0.00250	0.43
Parietal	0.4325 ± 0.0241	0.4327 ± 0.0028	0.4324 ± 0.0025	0.94	0.4365 ± 0.0025	0.4267 ± 0.0027	0.011
Occipital	0.3736 ± 0.0246	0.3770 ± 0.0028	0.3695 ± 0.0026	0.055	0.3754 ± 0.0027	0.3708 ± 0.0027	0.24
<i>Cortical Trace, mm<sup>2</sup>/sec</i>							
<i>Left Brain</i>							
Frontal	0.00227 ± 0.00012	0.002266 ± 0.00001	0.002266 ± 0.000010	0.97	0.002264 ± 0.000013	0.002269 ± 0.000014	0.77
Temporal	0.00244 ± 0.00012	0.002435 ± 0.00001	0.002444 ± 0.000010	0.61	0.002443 ± 0.000013	0.002434 ± 0.000013	0.65
Parietal	0.00234 ± 0.00013	0.002325 ± 0.00001	0.002352 ± 0.000010	0.24	0.002336 ± 0.000014	0.002344 ± 0.000014	0.71
Occipital	0.00221 ± 0.00011	0.002214 ± 0.00001	0.002195 ± 0.000010	0.29	0.002193 ± 0.000013	0.002224 ± 0.000012	0.10
<i>Right Brain</i>							
Frontal	0.00220 ± 0.00013	0.002204 ± 0.00001	0.002188 ± 0.000020	0.43	0.002182 ± 0.000014	0.002217 ± 0.000015	0.09

(continued on next page)

Table 1 (continued)

	Total (N = 163)	Females (N = 89)	Males (N = 74)	<i>p</i> <sub>sex</sub>	White adults (N = 97)	African American adults (N = 66)	<i>p</i> <sub>race</sub>
Temporal	0.00238 ± 0.00012	0.002376 ± 0.00001	0.002377 ± 0.000010	0.97	0.002388 ± 0.000013	0.002362 ± 0.000014	0.17
Parietal	0.00230 ± 0.00013	0.00230 ± 0.00001	0.002300 ± 0.000010	0.88	0.0023 ± 0.000014	0.002305 ± 0.000015	0.80
Occipital	0.00230 ± 0.00011	0.002301 ± 0.00001	0.002293 ± 0.000010	0.62	0.002299 ± 0.000013	0.002295 ± 0.000012	0.81
Intracranial volume, mm <sup>3</sup>	mean±SD 1,343,538 ± 140,976	mean±SE 1,263,697 ± 10,315	mean±SE 1,437,339 ± 14,704	<0.001	mean±SE 1,379,975 ± 14,356	mean±SE 1,287,492 ± 14,995	<0.001

Key: Age<sub>v1</sub>, age measured at HANDLS visit 1 (2004–2009);  $\delta$ NfL, Annualized rate of change in Neurofilament Light; dMRI, Diffusion Magnetic Resonance Imaging; FA, Fractional Anisotropy; HDL, High Density Lipoprotein; IQR, Interquartile Range; GM, Gray Matter; HANDLS, Healthy Aging in Neighborhoods of Diversity Across the Life Span; HANDLS-SCAN, Brain magnetic resonance imaging scan ancillary study of HANDLS; IQR, Interquartile range (25th–75th percentile); NfL, Neurofilament Light; TR, Trace; v<sub>1</sub>, visit 1 of HANDLS (2004–2009); v<sub>2</sub>, visit 2 of HANDLS (2009–2013); v<sub>scan</sub>, HANDLS-SCAN visit (2011–2015); WM, White Matter; WRAT-3, Wide Range Achievement Test, 3rd version.

<sup>a</sup> Values are Mean ± SD for totals and Mean ± SE for stratum-specific, or % (except for imputed data where it was Mean ± SE for totals). Volumes are expressed in mm<sup>3</sup>. *p*<sub>sex</sub> was obtained from *nd t*-tests for the unimputed covariates and from multinomial logit and linear regression models for the imputed data. Additional models with sex, race, age and poverty status were conducted to test whether the sex differences were independent other socio-demographic factors. All statistically significant sex and racial differences at type I error of 0.05 retained their statistical significance after further adjustment for age, race/sex and poverty status, except for those with a *b* superscript.

proach, Table S2 examined characteristics across NfL exposure tertiles, which are summarized in Online supplemental Result 1.

We tested whether NfL (Log<sub>e</sub> transformed) measured at v<sub>1</sub> (Tables 2 and S3) or v<sub>2</sub> (Tables 3) was associated with neuroimaging markers of brain aging, specifically WMI. The relationships were examined both overall and among men and women separately. In our minimally adjusted models (i.e., Model 1, adjusted for age, sex, race, poverty status, time of follow-up and ICV) we corrected for multiple testing (*q* < 0.05). In these models, we found that NfL<sub>v1</sub> was significantly associated with greater TR<sub>global</sub> ( $\beta \pm SE$ : + 0.0000560 ± 0.0000186, *b* = 0.27, *p* = 0.003, *q* = 0.012), at follow up v<sub>scan</sub> visit ~5–6 years later. In addition, NfL<sub>v1</sub> was also significantly associated with later TR in both left and right frontal WM (left frontal WM:  $\beta = 0.0000706 \pm 0.0000201$ , *b* ± 0.30, *p* = 0.001, *q* = 0.0093; right frontal WM:  $\beta = 0.0000767 \pm 0.000021$ , *b* ± 0.31, *p* < 0.001, *q* = 0.0093). This association was largely unaltered with addition of other covariates, including v<sub>1</sub> BMI (Table 2, Model 2), or other upstream potentially confounding variables including measures of kidney and liver disease (Table S3, Model 3–6). Interestingly, we found that the association between NfL and TR<sub>global</sub> was also only detected among males, without a significant interaction by sex (*p* > 0.10 for sex × NfL<sub>v1</sub> in unstratified models) in the BMI-adjusted model 2. The addition of upstream covariates did not affect the findings in males. (Table S3, Models 3–6). In contrast, a relationship with global WMI was not detected when examining a shorter follow up time (~1.1 years) between plasma NfL exposure at visit 2 and dMRI outcome, (Table 3)(i.e., FA<sub>global</sub>, TR<sub>global</sub>), overall or by sex.

Among secondary analyses (Table S4), we found that NfL at v<sub>1</sub> was associated with global TR among White adults, while NfL at v<sub>2</sub> was linked with global TR among African American adults. These effects were consistently greater in the frontal WM region in both groups and the left temporal WM region among African American adults (Model 1:  $\beta \pm SE$ : 0.0000556 ± 0.000022, *b* = 0.30, *p* = 0.014). Nevertheless, with few exceptions (e.g., frontal and temporal regions for NfL<sub>v2</sub> vs. TR), there was no significant heterogeneity detected across race in the relationship between NfL and WMI (*p*<sub>race×NfL</sub> > 0.10). Further adjustment for BMI and other lifestyle and health-related factors selected using machine learning techniques generally did not alter these main findings.

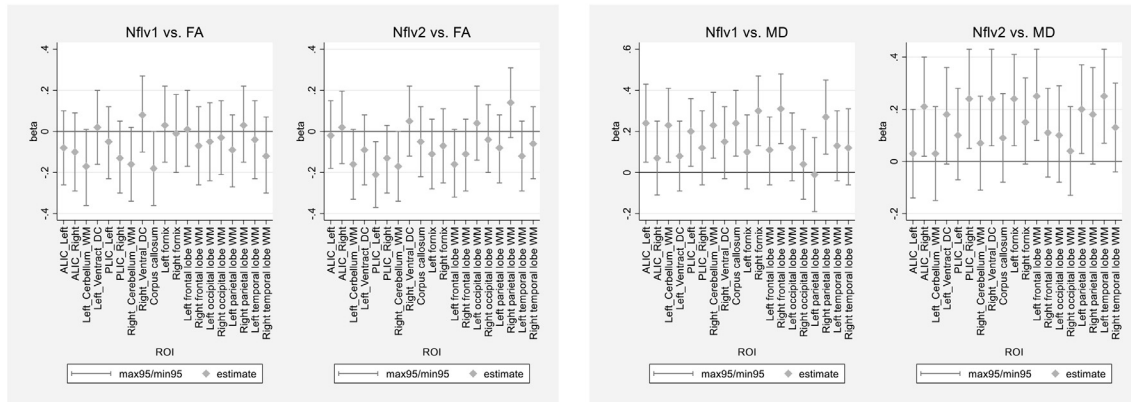
We also examined NfL levels over time in relation to WMI outcomes. In this analysis, we categorized NfL tracking over time (i.e., at v<sub>1</sub> and v<sub>2</sub>), or retaining a value either below or above the median (i.e., 8 pg/mL) in the overall sample, versus all oth-

ers (Table S5). “Tracking High” on NfL over time was associated with lower FA in some models, with the strongest effects detected in the left frontal WM region (Model 2: -0.0108 ± 0.0040, *p* = 0.009). Despite this association being robust to further adjustment for other covariates (Models 3–6), the relationship between “tracking high” on NfL and FA<sub>global</sub> was attenuated with addition of covariates associated with kidney/liver disease (Model 4) and lifestyle/health-related factors (Model 6). In contrast, “tracking low” on NfL was linked to lower TR<sub>global</sub> only in models adjusted for BMI (Model 2) and BMI+ diabetes (Model 3). The associations with left/right frontal, left occipital and right parietal WM TR regions were markedly attenuated between Models 2 and 3.

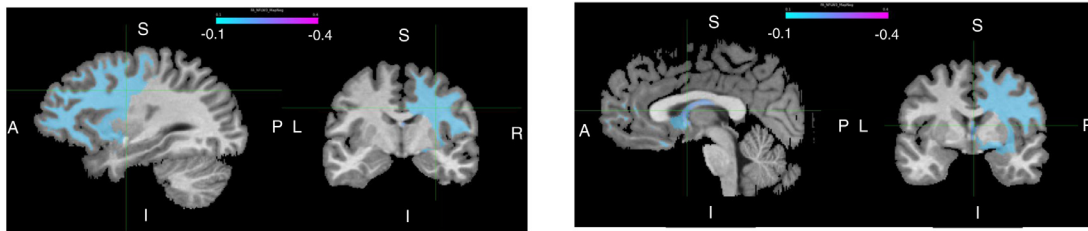
Our sensitivity analyses did not alter our main findings (*n* = 180, data not shown). Most notably, a 1 unit increase in NfL exposure at v<sub>1</sub> (Log<sub>e</sub> transformed) was associated with an increase in TR ( $\beta \pm SE$ : +0.0000574 ± 0.0000187) within the left frontal WM region (*p* = 0.002 in Model 1 (*b* = 0.336)). This association was not markedly attenuated in subsequent models. Consistent with this finding, there was a strong association between NfL<sub>v1</sub> and TR in the right frontal WM region (Model 1:  $\beta \pm SE$ : +0.0000775 ± 0.0000271, *p* = 0.005, *b* = 0.327). These findings remained in subsequent models and similar patterns of association were observed by sex. In race-specific models, patterns of associations were comparable. Most notably, among African American adults, NfL at v<sub>2</sub> was linked to greater TR within the left temporal WM region, even upon adjustment for BMI (Model 2:  $\beta \pm SE$ : +0.0000638 ± 0.0000187, *p* = 0.001, *n* = 79), an association not detected among White adults (*n* = 113).

ROI-specific findings are presented in Figure 2 and Table S6, examining the associations of NfL<sub>v1</sub> and NfL<sub>v2</sub> with mean diffusivity (or TR), in terms of effect sizes, 95% CI and *p*-values across 19 brain WM regions of interest. Results indicate that TR was directly associated with NfL<sub>v1</sub> within 11 of 19 ROIs (*p* < 0.05), with the leading ROIs having *p* < 0.010 including frontal WM (left and right), Ventral DC (left and right), temporal WM (right) and the Posterior Limb of the Internal Capsule or PLIC (right and left). NfL<sub>v1</sub> was not associated with any ROI-specific FA in this analysis. NfL<sub>v2</sub> was positively associated with 4 main ROI-specific TR, namely right and left fornix, left temporal lobe and corpus callosum. NfL<sub>v2</sub> was also inversely associated with FA within the right fornix and right frontal Lobe. All of our key findings presented in Tables 2 and 3, as well as Tables S3–S6, were largely unaltered in the sub-sample that was free from head injuries and was deemed as having normal cognition at v<sub>1</sub> based on MMSE scores (≥23).

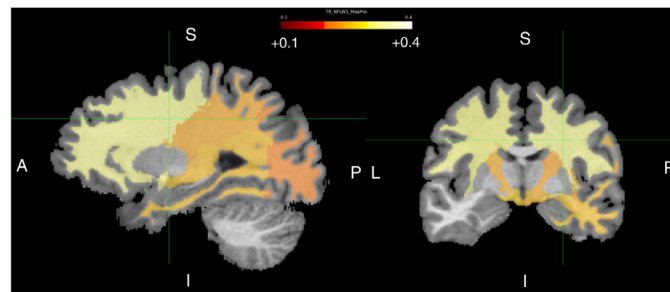
**(A) 95% CI for effect sizes of NfL at visits 1 or 2 vs. fractional anisotropies and mean diffusivities**



**(B) Fractional Anisotropy vs. visit 2 plasma Neurofilament Light Chain**



**(C) Mean Diffusivity vs. visit 1 plasma Neurofilament Light Chain**



**(D) Mean Diffusivity vs. visit 2 plasma Neurofilament Light Chain**

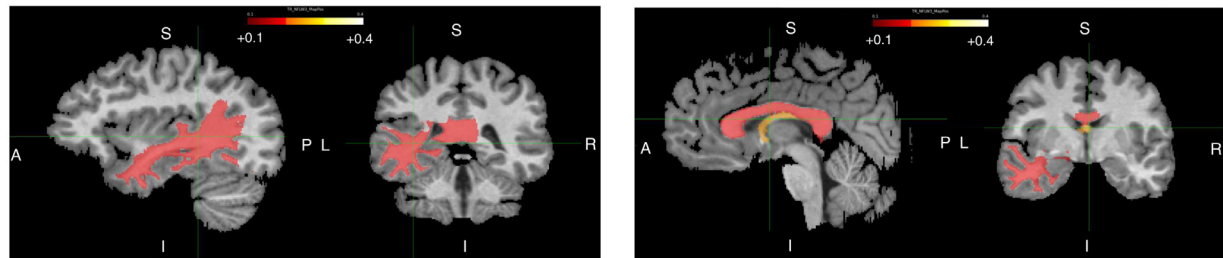


**Fig. 2.** A-D. Error bars and brain images of WMI measures [higher FA or lower MD (or TR)] versus  $\text{Log}_e$  transformed NfL<sub>v1</sub> and NfL<sub>v2</sub>; HANDLS 2004–2009/2009–2013 and HANDLS-SCAN 2011–2015<sup>a,b,c</sup>. *Abbreviations:* FA, Fractional Anisotropy; HANDLS, Healthy Aging in Neighborhoods of Diversity Across the Life Span; HANDLS-SCAN, HANDLS brain MRI ancillary study; MD, Mean Diffusivity; MRI, Magnetic Resonance Imaging; ROI, Region of Interest; WMI, White Matter Integrity. (A) In both the scatter plot and the brain images: Values are effect sizes from adjusted linear regression models with NfL<sub>v1</sub> and NfL<sub>v2</sub> ( $\text{Log}_e$  transformed and z-scored) as alternative exposures and outcomes being regional small ROI FA or MD. The  $\text{Log}_e$  transformed value was then z-scored. The error bar show the point estimate and its 95% CI (min95 and max95) of the  $b$  estimates. (B) The brain images represent the same results from 4 models, using FSLEYES software for visualizing effect sizes. Those effect sizes were selected for regions with  $p < 0.05$  and are presented at different thresholds presented by a color gradient ranging between 0.10 and 0.50 in absolute values. Colder (blue) colors are for negative associations (smaller FA with higher NfL exposure) and warmer colors (red through yellow) are for positive associations (larger MD with higher NfL exposure). Lighter colors indicate stronger effect sizes. Detailed results are presented in *supplemental Table 6*. The results for standardized regression coefficients are interchangeable between TR and MD (For interpretation of the references to color in this figure legend, the reader is referred to the Web version of this article.)

**Table 2**

Minimally and BMI-adjusted associations from analyses A (global mean FA and global mean TR) and A' (regional cortical FA/TR) versus visit 1 NfL (Log<sub>e</sub> transformed, overall and stratified by sex); ordinary least square analyses; HANDLS 2004–2009 and HANDLS-SCAN 2011–2015<sup>a</sup>

Total sample (N = 163)	Model 1: minimally adjusted					Model 2: BMI-adjusted, sensitivity analysis (SA) <sup>b</sup>			
	$\beta$ 1	(SE1)	b1	P1	q-value1	$\beta$ 2	(SE2)	P2	Interaction by sex
dMRI, Analysis A									
FA <sub>global</sub>	-0.003936	(0.0035556)	-0.103	0.27	—	-0.0044115	(0.0036995)	0.24	0.48
TR <sub>global</sub>	+0.0000560	(0.0000186)	+0.270	0.003	0.012	+0.0000434	(0.000019)	0.023	0.54
dMRI, Analysis A'									
Fractional anisotropy									
Left Frontal	-0.0056008	(0.0040428)	-0.125	0.17	—	-0.0060722	(0.0042072)	0.15	0.73
Left Temporal	-0.0014471	(0.0037188)	-0.037	0.70	—	-0.0015268	(0.0038721)	0.69	0.20
Left Parietal	+0.0005619	(0.0039374)	+0.013	0.89	—	+0.0012969	(0.0040939)	0.75	0.22
Left Occipital	+0.0015115	(0.0044781)	+0.032	0.74	—	+0.0002736	(0.004648)	0.95	0.85
Right Frontal	-0.0073231	(0.0042524)	-0.156	0.087	—	-0.0074757	(0.0044276)	0.093	0.99
Right Temporal	-0.004759	(0.0039467)	-0.120	0.23	—	-0.0060285	(0.0040917)	0.14	0.14
Right Parietal	-0.0031239	(0.0043035)	-0.069	0.47	—	-0.0039048	(0.0044749)	0.38	0.21
Right Occipital	-0.0006367	(0.0044579)	-0.014	0.89	—	-0.0019823	(0.0046241)	0.67	0.54
Trace									
Left Frontal	+0.0000706	(0.0000201)	+0.30	0.001	0.0093	+0.0000603	(0.0000207)	0.004	0.35
Left Temporal	+0.0000383	(0.000002)	+0.177	0.057	—	+0.0000201	(0.0000201)	0.32	0.79
Left Parietal	+0.0000433	(0.0000229)	+0.176	0.060	—	+0.0000284	(0.0000234)	0.23	0.70
Left Occipital	+0.0000267	(0.000020)	+0.124	0.19	—	+0.0000199	(0.0000208)	0.34	0.29
Right Frontal	+0.0000767	(0.000021)	+0.314	<0.001	0.0093	+0.0000628	(0.0000215)	0.004	0.31
Right Temporal	+0.0000571	(0.0000205)	+0.253	0.006	0.065	+0.0000455	(0.0000211)	0.033	0.83
Right Parietal	+0.0000575	(0.0000225)	+0.240	0.012	0.093	+0.0000479	(0.0000233)	0.041	0.91
Right Occipital	+0.0000449	(0.0000207)	+0.210	0.032	0.17	+0.0000341	(0.0000213)	0.11	0.61
Males (N = 74)									
dMRI, Analysis A									
FA <sub>global</sub>	-0.0008539	(0.0043663)	-0.026	0.85	—	-0.0012923	(0.0043966)	0.77	—
TR <sub>global</sub>	+0.0000572	(0.0000252)	+0.29	0.026	0.20	+0.0000531	(0.0000251)	0.038	—
dMRI, Analysis A'									
Fractional anisotropy									
Left Frontal	-0.0029532	(0.0049605)	-0.075	0.55	—	-0.0034719	(0.0049922)	0.49	—
Left Temporal	+0.0016152	(0.0048588)	+0.046	0.74	—	+0.0012584	(0.0049073)	0.80	—
Left Parietal	+0.0058711	(0.0044177)	+0.167	0.19	—	+0.0058925	(0.0044770)	0.19	—
Left Occipital	+0.0061423	(0.0058745)	+0.135	0.30	—	+0.0052632	(0.0058682)	0.37	—
Right Frontal	-0.0060154	(0.0052301)	-0.144	0.25	—	-0.0061491	(0.0052982)	0.25	—
Right Temporal	-0.0010423	(0.0049663)	-0.029	0.83	—	-0.0019114	(0.0049342)	0.70	—
Right Parietal	+0.0016373	(0.0050575)	+0.043	0.75	—	+0.0009931	(0.0050724)	0.85	—
Right Occipital	+0.0045926	(0.0053821)	+0.116	0.40	—	+0.0034776	(0.0053037)	0.51	—
Trace									
Left Frontal	+0.0000787	(0.0000255)	+0.370	0.003	0.099	+0.000075	(0.0000255)	0.005	—
Left Temporal	+0.0000375	(0.0000301)	+0.169	0.22	—	+0.0000322	(0.0000299)	0.29	—
Left Parietal	+0.0000417	(0.0000289)	+0.188	0.15	—	+0.0000374	(0.0000289)	0.20	—
Left Occipital	+0.0000333	(0.0000268)	+0.164	0.22	—	+0.0000307	(0.000027)	0.26	—
Right Frontal	+0.0000852	(0.0000278)	+0.369	0.004	0.099	+0.0000793	(0.0000273)	0.005	—
Right Temporal	+0.0000388	(0.0000266)	+0.202	0.11	—	+0.0000452	(0.0000294)	0.13	—
Right Parietal	+0.0000535	(0.0000285)	+0.248	0.065	—	+0.0000512	(0.0000287)	0.080	—
Right Occipital	+0.0000478	(0.0000291)	+0.217	0.11	—	+0.0000358	(0.0000267)	0.19	—
Females (N = 89)									
dMRI, Analysis A									
FA <sub>global</sub>	-0.0082394	(0.0059821)	-0.191	0.172	—	-0.0092182	(0.0065724)	0.17	—
TR <sub>global</sub>	+0.0000549	(0.000029)	+0.251	0.062	—	+0.0000314	(0.0000312)	0.31	—

Key: Age<sub>v1</sub>, age measured at HANDLS visit 1 (2004–2009);  $\delta$ NfL, Annualized rate of change in Neurofilament Light; Dmri, Diffusion Magnetic Resonance Imaging; FA, Fractional Anisotropy; GM, Gray Matter; IQR, Interquartile Range; HANDLS, Healthy Aging in Neighborhoods of Diversity Across the Life Span; HANDLS-SCAN, Brain magnetic resonance imaging scan ancillary study of HANDLS; HDL, High Density Lipoprotein; IQR=Interquartile range (25th HDL, High Density Lipoprotein; 75th percentile); NfL, Neurofilament Light; TR, Trace; v<sub>1</sub>, visit 1 of HANDLS (2004–2009); v<sub>2</sub>, visit 2 of HANDLS (2009–2013); v<sub>scan</sub>, HANDLS-SCAN visit (2011–2015); WM, White Matter; WRAT-3, Wide Range Achievement Test, 3rd version.

<sup>a</sup> Values are adjusted linear regression coefficients  $\beta$  with associated SE, standardized beta, uncorrected p-values, corrected q-values (false discovery rate) and results of sensitivity analysis. (N) is the sample size in each analysis. Standardized betas for NfL are computed as SD in outcome per SD in visit 1 NfL, Log<sub>e</sub> transformed. Q-values presented only for uncorrected p-values < 0.05 for model 1. Model 1 was adjusted for Age<sub>v1</sub>, sex, race, poverty status, intracranial volume and time of follow-up between visit 1 and v<sub>scan</sub>. Volumes are expressed in mm<sup>3</sup>.

<sup>b</sup> Model 2 is a sensitivity analysis further adjusting Model 1 for BMI after screening using machine learning techniques (See Supplemental methods 2).

#### 4. Discussion

This retrospective cohort study is among a few to examine the relationships of plasma NfL concentrations at 2 consecutive visits (v<sub>1</sub> and v<sub>2</sub>) with key diffusion brain MRI markers, including FA and TR, in a racially and socio-economically diverse sample of middle-aged urban adults. Therefore, our study is unique in that it was designed to be able to assess the effects of both race and

sex in a middle-aged cohort. Among key findings, in the overall sample of middle-aged urban adults, in ICV-corrected, socio-demographic factor and time of follow-up adjusted models, NfL<sub>v1</sub> was associated with greater TR<sub>global</sub>, and regional bilateral frontal WM TR at a follow-up period of 5–6 years. This association was strongest among male and White adults. Moreover, NfL at v<sub>2</sub> was consistently linked to greater TR in the left temporal WM region among African American adults. Consistently higher levels of NfL

**Table 3**  
Minimally and BMI-adjusted associations from analyses A (global mean FA and global mean TR) and A' (regional cortical FA/TR) versus visit 2 NFL (Log<sub>e</sub> transformed, overall and stratified by sex): ordinary least square analyses; HANDLS 2009–2013 and HANDLS-SCAN 2011–2015<sup>a</sup>

Total sample (N = 163)	Model 1: Minimally adjusted					Model 2: BMI-adjusted, sensitivity analysis (SA) <sup>b</sup>			
	$\beta$ 1	(SE1)	b1	P1	q-value1	$\beta$ 2	(SE2)	P2	Interaction by sex
dMRI, Analysis A									
FA <sub>global</sub>	-0.0046814	(0.0030288)	-0.133	0.12	—	-0.0048013	(0.0030573)	0.12	0.48
TR <sub>global</sub>	+0.0000242	(0.0000162)	+0.127	0.14	—	+0.0000188	(0.0000159)	0.24	0.54
Males (N = 74)									
dMRI, Analysis A									
FA <sub>global</sub>	-0.0038182	(0.0038953)	-0.126	0.33	—	-0.0035262	(0.0039212)	0.37	—
TR <sub>global</sub>	+0.0000297	(0.0000232)	+0.164	0.20	—	+0.0000336	(0.0000229)	0.15	—
Females (N=89)									
dMRI, Analysis A									
FA <sub>global</sub>	-0.0069487	(0.0052576)	-0.175	0.19	—	-0.0070028	(0.0053996)	0.20	—
TR <sub>global</sub>	+0.0000161	(0.0000259)	+0.080	0.54	—	3.79e-06	(0.0000257)	0.88	—

Key: Age<sub>v1</sub>, age measured at HANDLS visit 1 (2004–2009);  $\delta$ NfL, Annualized rate of change in Neurofilament Light; dMRI, Diffusion Magnetic Resonance Imaging; FA, Fractional Anisotropy; HDL, High Density Lipoprotein; IQR, Interquartile Range; GM, Gray Matter; HANDLS, Healthy Aging in Neighborhoods of Diversity Across the Life Span; HANDLS-SCAN, Brain magnetic resonance imaging scan ancillary study of HANDLS; IQR, Interquartile range (25th–75th percentile); NFL, Neurofilament Light; v<sub>1</sub>, visit 1 of HANDLS (2004–2009); v<sub>2</sub>, visit 2 of HANDLS (2009–2013); TR, Trace; v<sub>scan</sub>, HANDLS-SCAN visit (2011–2015); WM, White Matter; WRAT-3, Wide Range Achievement Test, 3rd version.

<sup>a</sup> Values are adjusted linear regression coefficients  $\beta$  with associated SE, standardized beta, uncorrected *p*-values, corrected *q*-values (false discovery rate) and results of sensitivity analysis. (N) is the sample size in each analysis. Standardized betas are computed as SD in outcome per SD in Nfl at v2. *Q*-values presented only for uncorrected *p*-values < 0.05 for model 1. Model 1 was adjusted for Age<sub>v1</sub>, sex, race, poverty status, intracranial volume and time of follow-up between visit 1 and v<sub>scan</sub>. Volumes are expressed in mm<sup>3</sup>.

<sup>b</sup> Model 2 is a sensitivity analysis further adjusting Model 1 for BMI at visit 1 after screening using machine learning techniques (See Supplemental methods 2).<sup>c</sup> *p* < 0.10 for null hypothesis that exposure  $\times$  sex 2-way interaction term is =0 in the unstratified model with exposure and sex included as main effects.

over time was associated with lower FA with the strongest effects detected in the left Frontal WM region. Although some of these findings were sex- and race-specific, there was little evidence of heterogeneity of effects across sex with only regional differences (mainly frontal and temporal) in effects detected across race for NflV<sub>2</sub> and TR.

#### 4.1. Previous human studies

Several studies have linked elevated plasma/serum Nfl with brain diffusion WMI markers in various neurological diseases. For example, in autosomal dominant mutation carriers for AD and patients with multiple sclerosis, elevated plasma/serum Nfl was associated with a decline in FA and increased mean, axial, and radial diffusivities in white matter (Al Shweiki et al., 2019; Schultz et al., 2020). In patients with behavioral variant frontotemporal dementia, higher plasma Nfl was associated with a reduction in FA in several sets of white matter tracts (Spotorno et al., 2020). Furthermore, in cerebrovascular diseases, increased serum Nfl levels were associated with higher TR in small vessel disease (Duering et al., 2018) and after ischemic stroke (Tiedt et al., 2018). These data suggest that in neurodegenerative diseases and in cerebrovascular disease that higher Nfl levels may indicate a reduction in connectivity in white matter regions. Additionally, while MD and/or TR are typically higher in damaged tissues as a result of increased free diffusion; FA decreases due to the loss of coherence in the main preferred diffusion direction (Soares et al., 2013). Most of findings with Nfl and WMI were in relation to increased TR and MD, particularly in the overall sample and for the baseline exposure (5–6 years prior to v<sub>scan</sub>). Thus, we can infer that higher Nfl at baseline is linked to free diffusion more so than incoherence in the main preferred diffusion direction. Nevertheless, tracking high over time in Nfl was also associated with reduced FA in the overall sample, suggesting that incoherence in the preferred diffusion direction can occur when Nfl is higher in a chronic manner.

Currently few studies have examined plasma Nfl in relation to diffusion brain MRI markers in individuals without dementia or cerebrovascular disease. In line with our findings though in

relation to a different fiber tract, higher plasma Nfl levels were associated with a decline in corpus callosum FA in non-demented older participants in the Mayo Clinic Study of Aging (Mielke et al., 2019). This study had a similar follow up period as our study from v<sub>1</sub> to v<sub>scan</sub> and also found similar effect sizes for Nfl measured in CSF and corpus callosum FA, which leads credence to the clinical utility of using plasma Nfl as a marker of non-specific neurodegeneration. In another study, dichotomizing Nfl into a low and high group found that individuals with high plasma Nfl had reduced FA in the posterior CC region with advancing age (Nyberg et al., 2020). In these studies, the effects of sex and race were not assessed. The fact that we observed a strong relationship in White adults between plasma Nfl and greater TR<sub>global</sub> is consistent with the findings from these all White older adult cohorts. Interestingly, we previously reported that initial Nfl level was associated with a faster decline on normalized mental status scores in White adults only (Beydoun et al., 2021). A recent study examining the association of various neuroimaging and clinical CSF markers of AD and comparing those relationships by race, found that cognitive impairment in African American adults is associated with smaller changes in CSF tau markers but greater impact from similar white matter hyper intensities (WMH) burden than Caucasians (Howell et al., 2017). The authors concluded that race-associated differences in CSF tau markers and ratios can lead to AD underdiagnoses among African American adults (Howell et al., 2017). Our findings also underscore the racial differences in the association between Nfl at different points in time in relation to regional mean diffusivities, as well as TR. Given that less WMI has been shown to precede greater accumulation of WMH (van Leijsen et al., 2018), our findings are comparable to the latter study. Specifically, we found that Nfl measured shortly prior to DTI assessment is linked to poorer WMI, consistently within the temporal region, among African American middle-aged adults, unlike among White adults for whom Nfl's relationship with global TR was detected when this blood biomarker was measured at least 5 years prior to DTI assessment. This finding suggests that Nfl's association with poor WMI, particularly higher TR, may be an acute one within the African American group, while requiring a longer period of

time to translate into adverse WMI outcomes among White adults. These differences in associations based on blood biomarker timing require further study through a replication in other comparable cohorts and the evaluation of underlying mechanisms behind those discrepancies.

Moreover, these data highlight the importance of studying racial differences in neuroimaging, cognitive and biomarker measures. This is particularly relevant given that African American adults in the United States bear a disproportionate burden of poor clinical brain health outcomes and higher prevalence and incidence of AD and related dementias (Mayeda et al., 2016). We are only beginning to understand the complex interplay of neurodegenerative markers, such as plasma NFL, and their relationship with race in the context of brain connectivity measurements.

#### 4.2. Strengths and limitations

The present study has several strengths, including a socioeconomically diverse sample of African American and White adults, a novel examination between markers of neuroaxonal damage and brain dMRI measures with up to 6 years of latency between NfL exposure and outcome (brain MRI measures) and the ability to assess longitudinal change in NfL and tracking high or low over time. Moreover, our study was sufficiently powered to examine sex and race differences in the exposures and outcomes of interest while accounting for a wide range of potential confounders, including sociodemographic, health, and lifestyle characteristics as well as numerous biomarkers. Furthermore, given the age range of our analytic sample, our study provides insight into the utility of plasma NfL for monitoring brain health of middle-aged adults.

The present study also has several limitations. As is common in observational studies, we are unable to rule out residual confounding despite our inclusion of a wide range of covariates. This includes, for example, the lack of a baseline dMRI measure. Second, the exposure-outcome associations observed in our analytic sample of middle-aged urban adults may not be generalizable to older adult populations. Third, despite the novelty of our approach, data limitations inhibit us from examining baseline exposures against annualized changes in our outcome. Moreover, the latency period between exposure and outcome differs among participants which we remedied by accounting for follow-up time in our models. Finally, despite conducting a sensitivity analysis among individuals free from suspected dementia at baseline, as determined by the MMSE score with a cutoff of 23, there is some degree of uncertainty regarding the sample being dementia-free given that no comprehensive assessment for dementia or its sub-types was available in HANDLS. The uncertainty around follow-up cognitive impairment, particularly dementia diagnosis, is an additional related limitation to this study.

#### 4.3. Conclusions

In summary, plasma NfL shows promise as a prognostic marker of future deficits in brain white matter integrity, particularly with respect to TR and MD, among middle-aged adults. The reliance on plasma NfL predictions depends on time and race as short-term follow up measurements were only associated with higher TR in African American adults. These data support the clinical utility of measuring blood NfL to monitor white matter integrity and warrant future studies to further validate this biomarker in middle-aged adults.

#### 4.4. Data availability statement

Data can be made available upon request to researchers with accepted proposals after completing the confidentiality agreement per request from our Institutional Review Board. Our policies are publicized on our website <https://handls.nih.gov>, which additionally contains the code book for the parent study, HANDLS. Data access may be requested from the PIs or the study manager, Jennifer Norbeck at [norbeckje@mail.nih.gov](mailto:norbeckje@mail.nih.gov). These data are owned by the National Institute on Aging at the National Institutes of Health. The PIs have restricted public access to these data for the following reasons: (1) The study collects medical, psychological, cognitive, and psychosocial information on racial and poverty differences that could be misconstrued or willfully manipulated to promote racial discrimination; and (2) although the sample is fairly large, there are sufficient identifiers that the PIs cannot guarantee absolute confidentiality for every participant as we have stated in acquiring our confidentiality certificate. Analytic scripts and code book specific to HANDLS SCAN can be obtained from the corresponding author upon request.

#### Credit author statement

MAB: Study concept, plan of analysis, data management, statistical analysis, literature search and review, write-up of parts of the manuscript, revision of the manuscript.

NNH: Study concept, plan of analysis, data acquisition, literature search and review, write-up of parts of the manuscript, revision of the manuscript.

JW: Plan of analysis, assistance with statistical analysis, literature search and review, write-up of parts of the manuscript, revision of the manuscript.

AIM: Plan of analysis, literature search and review, write-up of parts of the manuscript, revision of the manuscript.

HAB: Plan of analysis, assistance with statistical analysis, literature review, write-up of parts of the manuscript, revision of the manuscript.

LIK: Data acquisition, write-up of parts of the manuscript, revision of the manuscript.

CD: Data acquisition, write-up of parts of the manuscript, revision of the manuscript.

RPG: Data acquisition, write-up of parts of the manuscript, revision of the manuscript.

SLS: Data acquisition, write-up of parts of the manuscript, revision of the manuscript.

GE: Data acquisition, image analysis, assistance with statistical analysis, write-up of parts of the manuscript, revision of the manuscript.

MKE: Data acquisition, write-up of parts of the manuscript, revision of the manuscript.

ABZ: Data acquisition, plan of analysis, data management, write-up of parts of the manuscript, revision of the manuscript.

SRW: Data acquisition, plan of analysis, data management, literature search and review, write-up of parts of the manuscript, revision of the manuscript.

#### Disclosure statement

All authors declare no conflict of interest. The views expressed in this article are those of the authors and do not necessarily reflect the official policy or position of Fort Belvoir Community Hospital, the Defense Health Agency, Department of Defense, or U.S. Government. Reference to any commercial products within this publication does not create or imply any endorsement by Fort

Belvoir Community Hospital, the Defense Health Agency, Department of Defense, or U.S. Government.

## Acknowledgement

This study was supported by the Intramural Research Program of the National Institute on Aging, National Institutes of Health. The authors would like to thank all HANDLS and HANDLS SCAN participants, staff and investigators for their contributions to this study. The authors would like to thank Ms. Nicolle Mode for her contribution in selecting participants for plasma NfL analyses and related data management.

## Supplementary materials

Supplementary material associated with this article can be found, in the online version, at doi:[10.1016/j.neurobiolaging.2022.10.004](https://doi.org/10.1016/j.neurobiolaging.2022.10.004).

## References

2019. The 2004 HHS poverty guidelines. <https://aspe.hhs.gov/2004-hhs-poverty-guidelines> (Accessed September 2 2019).
- Al Shweiki, M.R., Steinacker, P., Oeckl, P., Hengerer, B., Danek, A., Fassbender, K., Diehl-Schmid, J., Jahn, H., Anderl-Straub, S., Ludolph, A.C., Schonfeldt-Lecuona, C., Otto, M., 2019. Neurofilament light chain as a blood biomarker to differentiate psychiatric disorders from behavioural variant frontotemporal dementia. *J Psychiatr Res* 113, 137–140. doi:[10.1016/j.jpsychires.2019.03.019](https://doi.org/10.1016/j.jpsychires.2019.03.019).
- Andersson, J.L.R., Sotiropoulos, S.N., 2016. An integrated approach to correction for off-resonance effects and subject movement in diffusion MR imaging. *Neuroimage* 125, 1063–1078. doi:[10.1016/j.neuroimage.2015.10.019](https://doi.org/10.1016/j.neuroimage.2015.10.019).
- Beydoun, M.A., Noren Hooten, N., Beydoun, H.A., Maldonado, A.I., Weiss, J., Evans, M.K., Zonderman, A.B., 2021. Plasma neurofilament light as a potential biomarker for cognitive decline in a longitudinal study of middle-aged urban adults. *Transl Psychiatry* 11 (1), 436. doi:[10.1038/s41398-021-01563-9](https://doi.org/10.1038/s41398-021-01563-9).
- de Wolf, F., Ghanbari, M., Licher, S., McRae-McKee, K., Gras, L., Weverling, G.J., Wermeling, P., Sedaghat, S., Ikram, M.K., Waziry, R., Koudstaal, W., Klap, J., Kostense, S., Hofman, A., Anderson, R., Goudsmit, J., Ikram, M.A., 2020. Plasma tau, neurofilament light chain and amyloid-beta levels and risk of dementia; a population-based cohort study. *Brain* 143 (4), 1220–1232. doi:[10.1093/brain/awaa054](https://doi.org/10.1093/brain/awaa054).
- Doshi, J., Erus, G., Ou, Y., Resnick, S.M., Gur, R.C., Gur, R.E., Satterthwaite, T.D., Furth, S., Davatzikos, C., Alzheimer's Neuroimaging, I., 2016. MUSE: Multi-atlas region segmentation utilizing ensembles of registration algorithms and parameters, and locally optimal atlas selection. *Neuroimage* 127, 186–195. doi:[10.1016/j.neuroimage.2015.11.073](https://doi.org/10.1016/j.neuroimage.2015.11.073).
- Duering, M., Konieczny, M.J., Tiedt, S., Baykara, E., Tuladhar, A.M., Leijssen, E.V., Lyrer, P., Engelter, S.T., Gesierich, B., Achmuller, M., Barro, C., Adam, R., Ewers, M., Dichgans, M., Kuhle, J., de Leeuw, F.E., Peters, N., 2018. Serum neurofilament light chain levels are related to small vessel disease burden. *J Stroke* 20 (2), 228–238. doi:[10.5853/jos.2017.02565](https://doi.org/10.5853/jos.2017.02565).
- Evans, M.K., Lepkowski, J.M., Powe, N.R., LaVeist, T., Kuczmarski, M.F., Zonderman, A.B., 2010. Healthy aging in neighborhoods of diversity across the life span (HANDLS): overcoming barriers to implementing a longitudinal, epidemiologic, urban study of health, race, and socioeconomic status. *Ethn Dis* 20 (3), 267–275.
- Hansson, O., Janelidze, S., Hall, S., Magdalinou, N., Lees, A.J., Andreasson, U., Norgren, N., Linder, J., Forsgren, L., Constantinescu, R., Zetterberg, H., Blennow, K., Swedish Bio, F.s., 2017. Blood-based NfL: A biomarker for differential diagnosis of parkinsonian disorder. *Neurology* 88 (10), 930–937. doi:[10.1212/WNL.0000000000003680](https://doi.org/10.1212/WNL.0000000000003680).
- He, L., de Souto Barreto, P., Aggarwal, G., Nguyen, A.D., Morley, J.E., Li, Y., Bateman, R.J., Vellas, B., Group, M.D., 2020. Plasma Aβeta and neurofilament light chain are associated with cognitive and physical function decline in non-dementia older adults. *Alzheimer's res ther* 12 (1), 128. doi:[10.1186/s13195-020-00697-0](https://doi.org/10.1186/s13195-020-00697-0).
- Howell, J.C., Watts, K.D., Parker, M.W., Wu, J., Kollhoff, A., Wingo, T.S., Dorbin, C.D., Qiu, D., Hu, W.T., 2017. Race modifies the relationship between cognition and Alzheimer's disease cerebrospinal fluid biomarkers. *Alzheimer's res ther* 9 (1), 88. doi:[10.1186/s13195-017-0315-1](https://doi.org/10.1186/s13195-017-0315-1).
- Jenkinson, M., Bannister, P., Brady, M., Smith, S., 2002. Improved optimization for the robust and accurate linear registration and motion correction of brain images. *Neuroimage* 17 (2), 825–841.
- Jenkinson, M., Smith, S., 2001. A global optimisation method for robust affine registration of brain images. *Med Image Anal* 5 (2), 143–156.
- Jones, D.K., 2008. Studying connections in the living human brain with diffusion MRI. *Cortex* 44 (8), 936–952. doi:[10.1016/j.cortex.2008.05.002](https://doi.org/10.1016/j.cortex.2008.05.002).
- Khalil, M., Pirpamer, L., Hofer, E., Voortman, M.M., Barro, C., Leppert, D., Benkert, P., Ropele, S., Enzinger, C., Fazekas, F., Schmidt, R., Kuhle, J., 2020. Serum neurofilament light levels in normal aging and their association with morphologic brain changes. *Nat Commun* 11 (1), 812. doi:[10.1038/s41467-020-14612-6](https://doi.org/10.1038/s41467-020-14612-6).
- Khalil, M., Teunissen, C.E., Otto, M., Piehl, F., Sormani, M.P., Gattringer, T., Barro, C., Kappos, L., Comabella, M., Fazekas, F., Petzold, A., Blennow, K., Zetterberg, H., Kuhle, J., 2018. Neurofilaments as biomarkers in neurological disorders. *Nat rev. Neurol* 14 (10), 577–589. doi:[10.1038/s41582-018-0058-z](https://doi.org/10.1038/s41582-018-0058-z).
- Mattsson, N., Cullen, N.C., Andreasson, U., Zetterberg, H., Blennow, K., 2019. Association longitudinal plasma neurofilament light and neurodegeneration in patients with Alzheimer disease. *JAMA Neurol* 76 (7), 791–799. doi:[10.1001/jamaneurol.2019.0765](https://doi.org/10.1001/jamaneurol.2019.0765).
- Mayeda, E.R., Glymour, M.M., Quesenberry, C.P., Whitmer, R.A., 2016. Inequalities in dementia incidence between six racial and ethnic groups over 14 years. *Alzheimers Dement* 12 (3), 216–224. doi:[10.1016/j.jalz.2015.12.007](https://doi.org/10.1016/j.jalz.2015.12.007).
- Mielke, M.M., Syrjanen, J.A., Blennow, K., Zetterberg, H., Vemuri, P., Skoog, I., Machulda, M.M., Kremers, W.K., Knopman, D.S., Jack Jr., C., Petersen, R.C., Kern, S., 2019. Plasma and CSF neurofilament light: Relation to longitudinal neuroimaging and cognitive measures. *Neurology* 93 (3), e252–e260. doi:[10.1212/WNL.0000000000007767](https://doi.org/10.1212/WNL.0000000000007767).
- Nyberg, L., Lundquist, A., Nordin Adolffsson, A., Andersson, M., Zetterberg, H., Blennow, K., Adolffsson, R., 2020. Elevated plasma neurofilament light in aging reflects brain white-matter alterations but does not predict cognitive decline or Alzheimer's disease. *Alzheimers Dement (Amst)* 12 (1), e12050. doi:[10.1002/dad2.12050](https://doi.org/10.1002/dad2.12050).
- Preische, O., Schultz, S.A., Apel, A., Kuhle, J., Kaeser, S.A., Barro, C., Graber, S., Kuder-Buletta, E., LaFougere, C., Laske, C., Voglein, J., Levin, J., Masters, C.L., Martins, R., Schofield, P.R., Rossor, M.N., Graff-Radford, N.R., Salloway, S., Ghetti, B., Ringman, J.M., Noble, J.M., Chhatwal, J., Goate, A.M., Benzinger, T.L.S., Morris, J.C., Bateman, R.J., Wang, G., Fagan, A.M., McDade, E.M., Gordon, B.A., Jucker, M., 2019. Serum neurofilament dynamics predicts neurodegeneration and clinical progression in presymptomatic Alzheimer's disease. *Nat Med* 25 (2), 277–283. doi:[10.1038/s41591-018-0304-3](https://doi.org/10.1038/s41591-018-0304-3).
- Rajan, K.B., Aggarwal, N.T., McAninch, E.A., Weuve, J., Barnes, L.L., Wilson, R.S., DeCarli, C., Evans, D.A., 2020. Remote blood biomarkers of longitudinal cognitive outcomes in a population study. *Ann neurol* 88 (6), 1065–1076. doi:[10.1002/ana.25874](https://doi.org/10.1002/ana.25874).
- Raket, L.L., Kuhnel, L., Schmidt, E., Blennow, K., Zetterberg, H., Mattsson-Carlgen, N., 2020. Utility of plasma neurofilament light and total tau for clinical trials in Alzheimer's disease. *Alzheimers Dement (Amst)* 12 (1), e12099. doi:[10.1002/dad2.12099](https://doi.org/10.1002/dad2.12099).
- Roalf, D.R., Gur, R.E., Verma, R., Parker, W.A., Quarmley, M., Ruparel, K., Gur, R.C., 2015. White matter microstructure in schizophrenia: associations to neurocognition and clinical symptomatology. *Schizophr Res* 161 (1), 42–49. doi:[10.1016/j.schres.2014.09.026](https://doi.org/10.1016/j.schres.2014.09.026).
- Rubsamen, N., Maceski, A., Leppert, D., Benkert, P., Kuhle, J., Wiendl, H., Peters, A., Karch, A., Berger, K., 2021. Serum neurofilament light and tau as prognostic markers for all-cause mortality in the elderly general population-an analysis from the MEMO study. *BMC Med* 19 (1), 38. doi:[10.1186/s12916-021-01915-8](https://doi.org/10.1186/s12916-021-01915-8).
- Scherling, C.S., Hall, T., Berisha, F., Klepac, K., Karydas, A., Coppola, G., Kramer, J.H., Rabinovici, G., Ahljianian, M., Miller, B.L., Seeley, W., Grinberg, L.T., Rosen, H., Meredith Jr., J., Boxer, A.L., 2014. Cerebrospinal fluid neurofilament concentration reflects disease severity in frontotemporal degeneration. *Annals of neurology* 75 (1), 116–126. doi:[10.1002/ana.24052](https://doi.org/10.1002/ana.24052).
- Schultz, S.A., Strain, J.F., Adedokun, A., Wang, Q., Preische, O., Kuhle, J., Flores, S., Keefe, S., Dincer, A., Ances, B.M., Berman, S.B., Brickman, A.M., Cash, D.M., Chhatwal, J., Cruchaga, C., Ewers, M., Fox, N.N., Ghetti, B., Goate, A., Graff-Radford, N.R., Hassenstab, J.J., Hornbeck, R., Jack Jr., C., Johnson, K., Joseph-Mathurin, N., Karch, C.M., Koeppe, R.A., Lee, A.K.W., Levin, J., Masters, C., McDade, E., Perrin, R.J., Rowe, C.C., Salloway, S., Saykin, A.J., Sperling, R., Su, Y., Villedaigne, V.L., Voglein, J., Weiner, M., Xiong, C., Fagan, A.M., Morris, J.C., Bateman, R.J., Benzinger, T.L.S., Jucker, M., Gordon, B.A., Dominantly Inherited Alzheimer, N., 2020. Serum neurofilament light chain levels are associated with white matter integrity in autosomal dominant Alzheimer's disease. *Neurobiol Dis* 142, 104960. doi:[10.1016/j.nbd.2020.104960](https://doi.org/10.1016/j.nbd.2020.104960).
- Shahim, P., Gren, M., Liman, V., Andreasson, U., Norgren, N., Tegner, Y., Mattsson, N., Andreasen, N., Ost, M., Zetterberg, H., Nelligard, B., Blennow, K., 2016. Serum neurofilament light protein predicts clinical outcome in traumatic brain injury. *Scientific reports* 6, 36791. doi:[10.1038/srep36791](https://doi.org/10.1038/srep36791).
- Shaked, D., Leibel, D.K., Katzel, L.I., Davatzikos, C., Gullapalli, R.P., Seliger, S.L., Erus, G., Evans, M.K., Zonderman, A.B., Waldstein, S.R., 2019. Disparities in diffuse cortical white matter integrity between socioeconomic groups. *Front Hum Neurosci* 13, 198. doi:[10.3389/fnhum.2019.00198](https://doi.org/10.3389/fnhum.2019.00198).
- Soares, J.M., Marques, P., Alves, V., Sousa, N., 2013. A hitchhiker's guide to diffusion tensor imaging. *Front Neurosci* 7, 31. doi:[10.3389/fnins.2013.00031](https://doi.org/10.3389/fnins.2013.00031).
- Spotorno, N., Lindberg, O., Nilsson, C., Landqvist Waldo, M., van Westen, D., Nilsson, K., Vestberg, S., Englund, E., Zetterberg, H., Blennow, K., Latt, J., Markus, N., Lars-Olof, W., Alexander, S., 2020. Plasma neurofilament light protein correlates with diffusion tensor imaging metrics in frontotemporal dementia. *PLoS One* 15 (10), e0236384. doi:[10.1371/journal.pone.0236384](https://doi.org/10.1371/journal.pone.0236384).
- STATA, 2019. *Statistics/Data Analysis: Release 16.0*. Stata Corporation, Texas.
- Teunissen, C.E., Dijkstra, C., Polman, C., 2005. Biological markers in CSF and blood for axonal degeneration in multiple sclerosis. *Lancet. Neurol* 4 (1), 32–41. doi:[10.1016/S1474-4422\(04\)00964-0](https://doi.org/10.1016/S1474-4422(04)00964-0).

- Tiedt, S., Duering, M., Barro, C., Kaya, A.G., Boeck, J., Bode, F.J., Klein, M., Dorn, F., Gesierich, B., Kellert, L., Ertl-Wagner, B., Goertler, M.W., Petzold, G.C., Kuhle, J., Wollenweber, F.A., Peters, N., Dichgans, M., 2018. Serum neurofilament light: A biomarker of neuroaxonal injury after ischemic stroke. *Neurology* 91 (14), e1338–e1347. doi:[10.1212/WNL.0000000000006282](https://doi.org/10.1212/WNL.0000000000006282).
- Tristan-Vega, A., Aja-Fernandez, S., 2010. DWI filtering using joint information for DTI and HARDI. *Med Image Anal* 14 (2), 205–218. doi:[10.1016/j.media.2009.11.001](https://doi.org/10.1016/j.media.2009.11.001).
- van Leijsen, E.M.C., Bergkamp, M.I., van Uden, I.W.M., Ghafoorian, M., van der Holst, H.M., Norris, D.G., Platel, B., Tuladhar, A.M., de Leeuw, F.E., 2018. Progression of white matter hyperintensities preceded by heterogeneous decline of microstructural integrity. *Stroke* 49 (6), 1386–1393. doi:[10.1161/STROKEAHA.118.020980](https://doi.org/10.1161/STROKEAHA.118.020980).
- Waldstein, S.R., Dore, G.A., Davatzikos, C., Katzel, L.L., Gullapalli, R., Seliger, S.L., Kouo, T., Rosenberger, W.F., Erus, G., Evans, M.K., Zonderman, A.B., 2017. Differential associations of socioeconomic status with global brain volumes and white matter lesions in african american and white adults: the HANDLS SCAN study. *Psychosom Med* 79 (3), 327–335. doi:[10.1097/PSY.0000000000000408](https://doi.org/10.1097/PSY.0000000000000408).
- Weston, P.S.J., Poole, T., O'Connor, A., Heslegrave, A., Ryan, N.S., Liang, Y., Drueyeh, R., Mead, S., Blennow, K., Schott, J.M., Frost, C., Zetterberg, H., Fox, N.C., 2019. Longitudinal measurement of serum neurofilament light in presymptomatic familial Alzheimer's disease. *Alzheimers Res Ther* 11 (1), 19. doi:[10.1186/s13195-019-0472-5](https://doi.org/10.1186/s13195-019-0472-5).